RESEARCH PAPER

Interaction of diltiazem with an intracellularly accessible binding site on Ca$_V$1.2

W Shabbir[1]*, S Beyl[1]*, EN Timin[1], D Schellmann[2], T Erker[2], A Hohaus[1], GH Hockerman[3] and S Hering[1]

[1]Department of Pharmacology and Toxicology, University of Vienna, Althanstrasse, Vienna, Austria, [2]Department of Medicinal Chemistry, University of Vienna, Althanstrasse, Vienna, Austria, and [3]Department of Medicinal Chemistry and Molecular Pharmacology, Purdue University, West Lafayette, IN, USA

BACKGROUND AND PURPOSE

Diltiazem inhibits Ca$_V$1.2 channels and is widely used in clinical practice to treat cardiovascular diseases. Binding determinants for diltiazem are located on segments IIIS6, IVS6 and the selectivity filter of the pore forming α_1 subunit of Ca$_V$1.2. The aim of the present study was to clarify the location of the diltiazem binding site making use of its membrane-impermeable quaternary derivative d-*cis*-diltiazem (qDil) and mutant α_1 subunits.

EXPERIMENTAL APPROACH

Ca$_V$1.2 composed of α1, α2-δ and β2a subunits were expressed in tsA-201 cells and barium currents through Ca$_V$1.2 channels were recorded using the patch clamp method in the whole cell configuration. qDil was synthesized and applied to the intracellular side (via the patch pipette) or to the extracellular side of the membrane (by bath perfusion).

KEY RESULTS

Quaternary derivative d-*cis*-diltiazem inhibited Ca$_V$1.2 when applied to the intracellular side of the membrane in a use-dependent manner (59 $\pm$ 4% at 300 μM) and induced only a low level of tonic (non-use-dependent) block (16 $\pm$ 2% at 300 μM) when applied to the extracellular side of the membrane. Mutations in IIIS6 and IVS6 that have previously been shown to reduce the sensitivity of Ca$_V$1.2 to tertiary diltiazem also had reduced sensitivity to intracellularly applied qDil.

CONCLUSION AND IMPLICATIONS

The data show that use-dependent block of in Ca$_V$1.2 by diltiazem occurs by interaction with a binding site accessible via a hydrophilic route from the intracellular side of the membrane.

Abbreviations

Dil, d-*cis*-diltiazem; qDil, quaternary derivative of d-*cis*-diltiazem; SQ32, 428, quaternary benzothiazepine [(cis)-1,3,4,5-tetrahydro-4-(4-methoxyphenyl)-3-methyl-6- (trifluoromethyl)-1-[2-trimethylammonio)ethyl]-2H-1-benzazepin-2-o ne]

Introduction

L-type calcium channels belong to the high-voltage-activated channel family (isoforms Ca$_V$1.1, Ca$_V$1.2, Ca$_V$1.3 and Ca$_V$1.4) and display a high sensitivity to calcium channel blockers (or Ca^{2+} antagonists) (Catterall *et al.*, 2005). Ca$_V$1.2 participates in excitation–contraction coupling in cardiac and smooth muscle, action potential propagation in sinoatrial and

atrioventricular node, synaptic plasticity and hormone secretion and other processes (Striessnig, 1999; Catterall, 2000; Schulla *et al.*, 2003; Sinnegger-Brauns *et al.*, 2004). Calcium antagonists are widely used to treat cardiovascular diseases such as hypertension, angina pectoris and arrhythmias (Striessnig, 1999; Triggle, 2007). They are a chemically heterogeneous group of drugs that exert their therapeutic effects by inhibiting voltage-gated L-type Ca^{2+} channels. The prototypical agents of this group are diltiazem (Dil; a benzothiazepinone, BTZ), nifedipine (a 1,4-dihydropyridine, DHP) and verapamil (a phenylalkylamine, PAA). Single amino acids determining the sensitivity of L-type channels for calcium antagonists have been identified by mutational analysis and functional studies (Hering *et al.*, 1996; Kraus *et al.*, 1998; Striessnig *et al.*, 1998, Berjukow *et al.*, 1999 Hockerman *et al.*, 2000; Dilmac *et al.*, 2003).

The binding sites for PAA and diltiazem share common amino acid residues but it is assumed that the two classes of drug access their binding pockets from different sides of the membrane. There is clear evidence from studies with quaternary PAA analogues applied via the patch pipette that this class of $Ca_V1.2$ inhibitors interacts with an intracellular located binding site (Hescheler *et al.*, 1982; Berjukov *et al.*, 1996). Thus it is widely believed that tertiary PAAs penetrate the membrane and block $Ca_V1.2$ from the cytosolic side of the membrane in their protonated form in a use-dependent manner. $Ca_V1.2$ inhibition by diltiazem is also use-dependent (Lee and Tsien, 1983; Uehara and Hume, 1985; Smirnov and Aaronson, 1998). Variation of external and internal pH revealed that diltiazem inhibits L-type channels in its charged and neutral forms (Smirnov and Aaronson, 1998). Studies with a structurally related benzothiazepine [quaternary benzothiazepine [(cis)-1,3,4,5-tetrahydro-4-(4-methoxyphenyl)-3-methyl-6-(trifluoromethyl)-1-[2-trimethylammonio)ethyl]-2H-1-benzazepin-2-o ne] (SQ32,428)] suggested, however, an extracellular location of the diltiazem binding site (Hering *et al.*, 1993). The latter finding is in apparent contradiction with mutational studies indicating that crucial diltiazem binding determinants overlap with determinants of PAA sensitivity located deeply in the channel pore (Hering *et al.*, 1996; Kraus *et al.*, 1998; Berjukow *et al.*, 1999; Hockerman *et al.*, 2000; Dilmac *et al.*, 2003). Tikhonov and Zhorov (2008) pointed out that the potential BTZ binding determinants are located in the inner pore of Cav1.2 while some quaternary BTZ block the channel when applied externally rather than internally. The authors proposed a molecular model explaining the interaction with key amino acids of the putative binding pocket that were identified in functional studies. Tikhonov and Zhorov (2008) suggest that drug access occurs via the III/IV domain interface from the outside of the membrane.

However, to date no study has systematically examined the extracellular and intracellular action of the therapeutically used diltiazem on $Ca_V1.2$. Therefore we synthesized the quaternary derivative of d-*cis*-diltiazem, qDil, and explored its effects when applied from outside or inside (via the patch pipette) of the cell membrane. Our data on wild-type and mutant $Ca_V1.2$ clearly demonstrate 'use-dependent' intracellular access of qDil to the diltiazem binding pocket in $Ca_V1.2$.

Methods

All chemicals obtained from commercial suppliers were used as received and were of analytical grade. Melting points were determined on a Kofler hot stage apparatus and are uncorrected. The ^1H- and ^{13}C-NMR spectra were recorded on a Bruker Avance DPx200 (200 and 50 MHz).

Synthesis of quaternary diltiazem

Iodomethane, 0.568 g (4 mmol), was added to a solution of the free base of 0.829 g (2 mmol) diltiazem in 2 mL dichloromethane at room temperature. After 48 h the reaction mixture was concentrated to dryness. The crude product of qDil was obtained and recrystallized from isopropanol to yield 0.807 g (97%) of qDil.

The analysis of this material gave the following results: Mp 178–181°C; ^1H-NMR (D_2O): δ 7.68–7.64 (m, 3H), δ 7.38–7.26 (m, 3H), δ 6.89 ($J_{A,B}$ = 8.58 Hz, 2H), δ 5.04 (q, 2H), δ 4.13–4.08 (m, 1H), δ 3.96–3.83 (m, 2H), δ 3.72 (s, 4H), δ 3.42–3.38 (m, 1H), δ 3.09 (s, 9H), δ 1.80 (s, 3H); ^{13}C-NMR (D_2O): δ 170.29, δ 169.10, δ 160.28, δ 144.35, δ 136.24, δ 132.83, δ 131.02, δ 128.92, δ 127.65, δ 126.32, δ 125.63, δ 114.36, δ 71.85, δ 63.47, δ 55.74, δ 54.61, δ 50.10, δ 44.54, δ 20,89.

The purity of qDil was confirmed by high-performance liquid chromatography and was 98%. The analysis was performed using a Jasco UV-1575 Chromatograph. The stationary phase was a 5 μm RP-18e Lichrospher Merck column (250 mm × 4 mm). As a mobile phase, ammonium acetate pH 6.0 + 0.5% DEA/CAN (50/50) was used.

Cell culture and transient transfection

Human embryonic kidney tsA-201 cells were grown at 5% CO2 and 37°C to 80% confluence in Dulbecco's modified Eagle's medium/F-12 supplemented with 10% (v·v^{-1}) fetal calf serum and 100 units·mL^{-1} of penicillin and streptomycin. Cells were split using trypsin/EDTA and plated on 35 mm Petri dishes (Falcon, Franklin Lakes, NJ, USA) at 30–50% confluence 16 h before transfection. Subsequently, tsA-201 cells were co-transfected with cDNAs encoding wild-type (GenBankTM accession number X15539) or mutant $Ca_V1.2$ α1-subunits (I1150A, I1153A, I1156A, M1160A, F1164A, V1165A, I1460A, I1464A, Y1463F, F1117G, E1118Q, E1419Q; Hockerman *et al.*, 2000) with auxiliary β$_{2a}$, α$_2$δ subunits (Ellis *et al.*, 1988). The transfection of tsA-201 cells was performed using the FuGENE 6 transfection reagent (Roche Applied Science, Indianapolis, IN, USA) following standard protocols.

Ionic current recordings and data acquisition

Barium currents (I_{Ba}) through voltage-gated Ca^{2+} channels were recorded at 22–25°C using the whole cell patch-clamp configuration (Hamill *et al.*, 1981) by Axopatch 200A patch clamp amplifier (Axon Instruments, Union City, CA, USA) 36–48 h after transfection. The extracellular bath solution contained 20 mM $BaCl_2$, 1 mM $MgCl_2$, 10 mM HEPES and 140 mM choline-Cl, titrated to pH 7.4 with methanesulphonic acid. The borosilicate glass patch pipettes (HARVARD APPARATUS, Holliston, MA, USA) with resistances of 1–4 MΩ were pulled and polished using a DMZ universal puller (Zeitz Instruments, Martinsried, Germany), and were filled with

Table 1

Peak current decay in the absence of drug after 20 pulses (100 ms) at 0.2 Hz

Mutation	Control inhibition, %
Wild-type	5.9 ± 3.0
I1150A	3.6 ± 1.5
I1153A	9.9 ± 2.1
I1156A	9.3 ± 1.8
M1160A	14.8 ± 1.6
F1164A	10.1 ± 3.3
V1165A	0.7 ± 1.8
I1460A	10.6 ± 0.9
Y1463F	0.9 ± 1.2
M1464A	0.7 ± 3.0
F1117G	9.5 ± 1.2
E1118Q	9.2 ± 1.8
E1419Q	3.6 ± 4.8

pipette solution containing 145 mM CsCl, 3 mM MgCl$_2$, 10 mM HEPES and 10 mM EGTA, titrated to pH 7.25 with CsOH.

Intracellular application was done via the patch pipettes and I_{Ba} were recorded 5 min after the whole cell configuration was established. To ensure that the internal drug concentration reached steady state, use-dependent block was monitored after different time intervals. An approximation of the time for intracellular perfusion (Mathias *et al.*, 1990) predicts that under our experimental conditions, an equilibrium between the pipette concentration of qDil and the intracellular solution should be reached within about 10 s.

For extracellular application, the drug was applied to cells under voltage clamp using a microminifold perfusion system (ALA scientific Instruments, Westbury, NY, USA). I_{Ba} were recorded by applying repetitive pulses after a 5 min equilibration period in drug-containing solution. Use-dependent Ca^{2+} channel block was estimated as peak I_{Ba} inhibition during a train of short (100 ms) test pulses from −80 mV at a frequency of 0.2 Hz. The dose–response curves of I_{Ba} inhibition were fitted using the Hill equation, $\frac{I_{Ba,drug}}{I_{Ba,control}}(in\%) = \frac{100 - A}{1 + \left(\frac{C}{IC_{50}}\right)^{nH}} + B$, where IC$_{50}$ is the concentration at which I_{Ba} inhibition is half-maximal, C is the applied drug concentration, B represents a non-blocked current and A the blocked current fraction (both in per cent). Channel block levels observed in the presence of drug were corrected by subtracting the mean steady-state inhibition (after 20 pulses, see Table 1) in controls. All data were digitized using a DIGIDATA 1200 interface (Axon Instruments), smoothed by means of a 4-pole Bessel filter, and stored on computer hard disc. Leak currents were subtracted digitally using average values of scaled leakage currents elicited by a 10 mV hyperpolarizing pulse. Series resistance and offset voltage were routinely compensated. The pClamp software package (version

7.0 Axon Instruments Inc.) was used for data acquisition and preliminary analysis.

The voltage-dependence of activation was determined from current–voltage (I-V) curves in the absence and presence of drug. The curves were fitted according to the following modified Boltzmann term:

$$I = \frac{G_{max} \cdot (V - V_{rev})}{1 + \exp\frac{V_{0.5,act} - V}{k_{act}}}$$

where V_{rev}, extrapolated reversal potential; V, membrane potential; I, peak current; G_{max}, maximum membrane conductance; $V_{0.5, act}$, voltage for half-maximal activation; and k_{act}, slope factor.

The voltage-dependence of I_{Ba} inactivation (inactivation curve) in the presence and absence of drug was measured using a multistep protocol (see Hohaus *et al.*, 2005). In order to avoid accumulation of channel block, the pulse sequence was applied every 2 min from a holding potential of −80 mV. Inactivation curves were drawn according to a Boltzmann equation:

$$I_{Ba,inactivation} = I_{SS} + \frac{1 - I_{SS}}{1 + \exp\frac{V - V_{0.5,inact}}{k_{inact}}}$$

where V, membrane potential; $V_{0.5,inact}$, midpoint voltage; k_{inact}, slope factor and I_{ss}, fraction of non-inactivating current.

Recovery from block was monitored by applying six short (20 ms) test pulses after the conditioning train. Application of the monitoring pulses in the presence of 300 μM of the used drugs did not induce measurable channel inhibition.

Analysis and curve fitting was performed with Microcal Origin 7.0. Data are given as mean ± SE. Statistical significance was assessed using Student's unpaired *t*-test.

Results

To clarify the interaction of diltiazem with either an extra- or intracellular binding site on Ca$_V$1.2, the membrane-impermeable qDil was synthesized (see *Methods*). Ca$_V$1.2 composed of wild-type or mutant α1 subunits and auxiliary α2-δ and β2a subunits were expressed in tsA 201 cells. qDil was applied intracellularly via the patch pipette and extracellularly in the perfusion bath.

Quaternary Dil blocks Ca$_V$1.2 when applied to the intracellular side and had only weak effects when applied to the extracellular side of the membrane

As shown in Figure 1A, qDil blocked I_{Ba} in a use-dependent manner when applied via the patch pipette. I_{Ba} inhibition was induced by applying a train of 100 ms test pulses from −80 mV to 20 mV at a frequency of 0.2 Hz. Figure 1C and D illustrates the acceleration of the current decay (statistically not significant) during the first pulse. Current traces from control cells and first pulse currents of a train with qDil in the pipette were normalized and averaged. The direct comparison of control I_{Ba} and I_{Ba} in the presence of drug was not possible under these conditions.
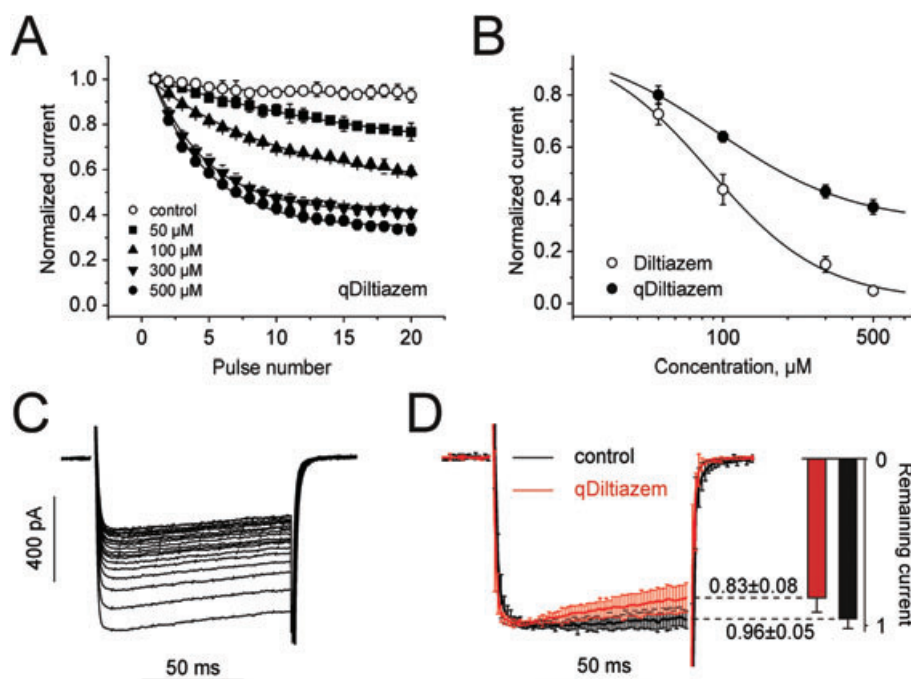
Figure 1

Use-dependent block of $Ca_V1.2$ by intracellularly applied quaternary diltiazem. (A) Use-dependent inhibition of wild-type channels measured in the absence or presence of 50, 100, 300 or 500 µM quaternary diltiazem in the intracellular (pipette) solution. Data points are the mean from 4–6 experiments. (B) The IC_{50} values [d-*cis*-diltiazem: 95 ± 5 µM (Hill slope $n_H = 1.6 \pm 0.4$) and quaternary derivative of d-*cis*-diltiazem (qDil): 85 ± 9 µM ($n_H = 1.3 \pm 0.2$)] were obtained by fitting the data points to the Hill equation (as described in Methods). Channel block was estimated as peak I_{Ba} inhibition during trains of 20 pulses (0.2 Hz, 100 ms) applied from a holding potential of −80 mV to +20 mV in control (Table 1) and in the presence of quaternary diltiazem. (C) Superimposed I_{Ba} during a train of 20 pulses with 300 µM quaternary diltiazem in pipette. (D) Acceleration of current decay during the first pulse in train. Current traces were normalized and averaged. The mean peak current densities were -14.7 ± 0.9 (control) and -13.8 ± 0.9 pA·pF^{-1} (first pulse current after 3 min of 300 µM qDil in the pipette). Histograms indicate remaining current at the end of the first pulse.

In order to evaluate potential resting state inhibition by qDil from the intracellular side, we compared the peak current densities in control and after a 3-min intracellular application of qDil (300 µM). The mean peak current densities of -14.7 ± 0.9 (control) and -13.8 ± 0.9 pA·pF^{-1} (calculated from first pulse I_{Ba} with 300 µM qDil in the pipette) suggest that qDil when applied from the intracellular side of the membrane only induces non-significant resting state inhibition. We cannot exclude the possibility that the reduced peak current density reflects open channel inhibition developing during the rising phase of current.

The kinetics of peak current inhibition during pulse trains and the final steady-state values were dependent on qDil concentration. The steady-state values plotted versus the applied drug concentrations are shown in Figure 1B. The IC_{50} values for I_{Ba} inhibition of wild-type $Ca_V1.2$ by qDil and Dil were 95 ± 5 µM and 85 ± 9 µM respectively (Figure 1B).

Extracellular application of 300 µM qDil induced $10 \pm 4\%$ use-dependent I_{Ba} inhibition of wild-type $Ca_V1.2$ (Figure 2A and B), which was not significantly different from the current decay during a pulse train in the absence of drug ($6 \pm 3\%$). The same drug concentration induced $59 \pm 4\%$ inhibition of I_{Ba} when applied via the pipette, indicating that qDil accesses its binding site on $Ca_V1.2$ from the intracellular side of the membrane (Figure 1B).

The tonic block of I_{Ba} (current inhibition after 3 min in drug at rest) induced by 100 and 300 µM Dil and qDil is shown in Figure 2D. Neither 100 nor 300 µM of qDil induced substantial I_{Ba} inhibition ($12 \pm 2\%$ and $16 \pm 2\%$ respectively). This block was not enhanced by repetitive pulsing. Extracellularly applied Dil induced larger tonic current inhibition than qDil, which can be prescribed to channel inhibition by the neutral form of the drug (see Smirnov and Aaronson, 1998).

Intracellularly applied 300 µM SQ32,428 (a quaternary benzothiazepine, see also Hering *et al.*, 1993) induced minimal channel inhibition (Figure 2C). The structures of qDil and SQ32,428 are compared in Figure 2B. Externally applied SQ32,428 (100 and 300 µM) inhibited I_{Ba} by $23 \pm 2\%$ ($n = 5$) and $43 \pm 3\%$ ($n = 5$), respectively, in a non-use-dependent manner (Figure 2D, see Hering *et al.*, 1993 for similar experiments on BC3H1 cells).

qDil interaction with the diltiazem binding site

Six amino acid residues on segment IIIS6 and three residues on segment IVS6 (Figure 3A) of the $Ca_V1.2$ α1 subunit have been shown to affect channel inhibition by Dil (Hering *et al.*, 1996; Hockerman *et al.*, 2000; Dilmac *et al.*, 2003). To elucidate whether its quaternary derivative interacts with the same binding pocket, we first studied I_{Ba} inhibition in IIIS6 mutants
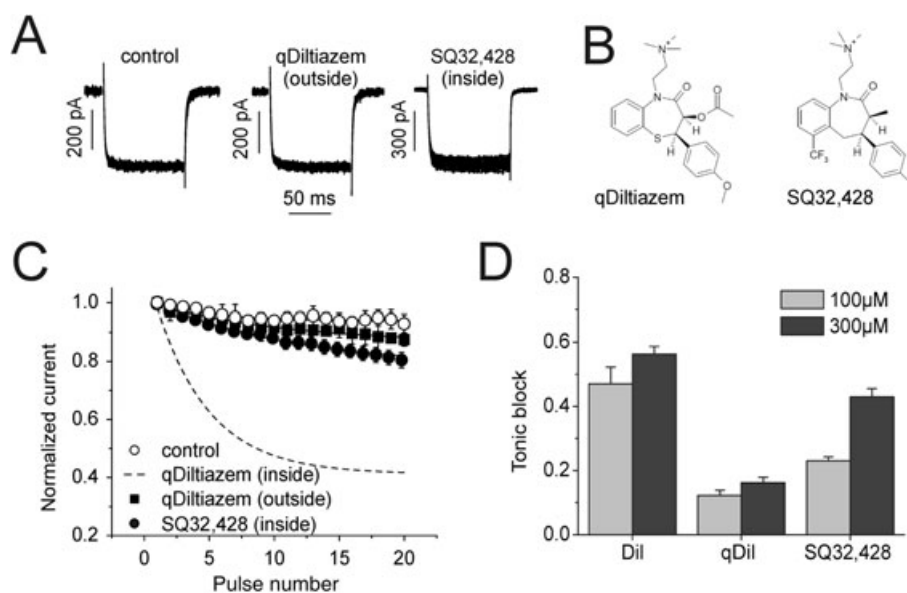
Figure 2

Extracellular quaternary diltiazem and intracellular [quaternary benzothiazepine [(cis)-1,3,4,5-tetrahydro-4-(4-methoxyphenyl)-3-methyl-6-(trifluoromethyl)-1-[2-trimethylammonio)ethyl]-2H-1-benzazepin-2-o ne] (SQ32,428)] do not inhibit Ca$_V$1.2. (A) Superimposed I_{Ba} during a train of 20 pulses (same protocol as in Figure 1) in the absence of drug, with 300 μM quaternary diltiazem in the bath solution and with 300 μM SQ32,428 in pipette. (B) Structures of quaternary diltiazem and benzothiazepinone SQ32,428. (C) Lack of significant I_{Ba} inhibition by extracellularly applied quaternary derivative of d-*cis*-diltiazem (qDil) (300 μM) and intracellularly applied SQ32,428 (300 μM). Peak current decay with 300 μM qDil in the pipette is shown for comparison as a broken line (data from Figure 1A). Data points are the mean from 4–6 experiments. (D) Illustrates tonic I_{Ba} inhibition (block after 3 min in drug at rest at –80 mV) induced by 100 and 300 μM Dil, d-*cis*-diltiazem (Dil) and SQ32,428 applied extracellularly.

I1150A, I1153A, I1156A, M1160A, F1164A and V1165A by intracellularly applied qDil. Three mutants (I1150A, F1164A, V1165A) significantly reduced sensitivity for qDil (Figure 3B and C), which is in line with their strong effects on Dil sensitivity (Hockerman *et al.*, 2000). The other mutations induced moderate (not statistically significant) effects, which might reflect the different experimental conditions. Rare pulsing every 20 s (0.05 Hz) from –60 mV induces predominantly tonic block (Hockerman *et al.*, 2000), while frequent pulsing every 5 s (0.2 Hz) induces predominantly use-dependent block (present study). Mutations of the key determinants of Dil sensitivity in segment IVS6 (I1460A, Y1463F and M1464A, Hockerman *et al.*, 2000) all significantly reduced qDil sensitivity (Figure 3D and E). To determine a possible interaction of qDil with potential binding sites in the selectivity filter, we analysed I_{Ba} inhibition of mutants F1117G, E1118Q and E1419Q. A moderate reduction in block compared with wild-type was observed (Figure 3F and G), which is in line with the results from a study by Dilmac *et al.* (2003).

Modulation of channel gating by quaternary and tertiary diltiazem

To obtain insights into the link between state-dependent inhibition and channel gating, we measured the standard characteristics of channel gating in control conditions and in the presence of a drug. The activation and inactivation curves are shown in Figure 4. Neither Dil (extracellular application) nor qDil (intracellular application) affected the activation

curve of Ca$_V$1.2 (Figure 4A, Table 2) and neither of them affected the kinetics of current activation and deactivation (data not shown). In line with previous studies, we observed a leftward shift of the inactivation curve by 300 μM Dil (5.0 ± 1.5 mV). Quaternary diltiazem applied at the same concentration from the intracellular side induced a very similar shift (7.1 ± 1.3 mV) suggesting similar state-dependency of both compounds (Figure 4B).

Recovery from block by qDil and Dil was compared at a holding potential of –80 mV. Figure 5 illustrates the very similar recovery from block by intracellular qDil and extracellularly applied Dil [τ(qDil) = 37.1 ± 4.9 s vs. τ(Dil) = 32.3 ± 5.2 s].

Discussion

Ca$_V$1.2 displays a high sensitivity to calcium antagonists such as DHPs, PAAs and diltiazem (Striessnig *et al.*, 1991; Hockerman *et al.*, 1997; Catterall *et al.*, 2005). Calcium antagonists are used clinically to treat hypertension and angina pectoris (Fleckenstein and Fleckenstein-Grun, 1980, Triggle, 2007) PAAs and diltiazem are also used as anti-arrhythmics and block L-type (Ca$_V$1.2) channels more efficiently at higher frequencies (Lee and Tsien, 1983).

Putative diltiazem binding determinants were identified on pore forming segments IIIS6 and IVS6 and the selectivity filter region (Hering *et al.*, 1996; Kraus *et al.*, 1998; Berjukow *et al.*, 1999; Hockerman *et al.*, 2000; Dilmac *et al.*, 2003). A
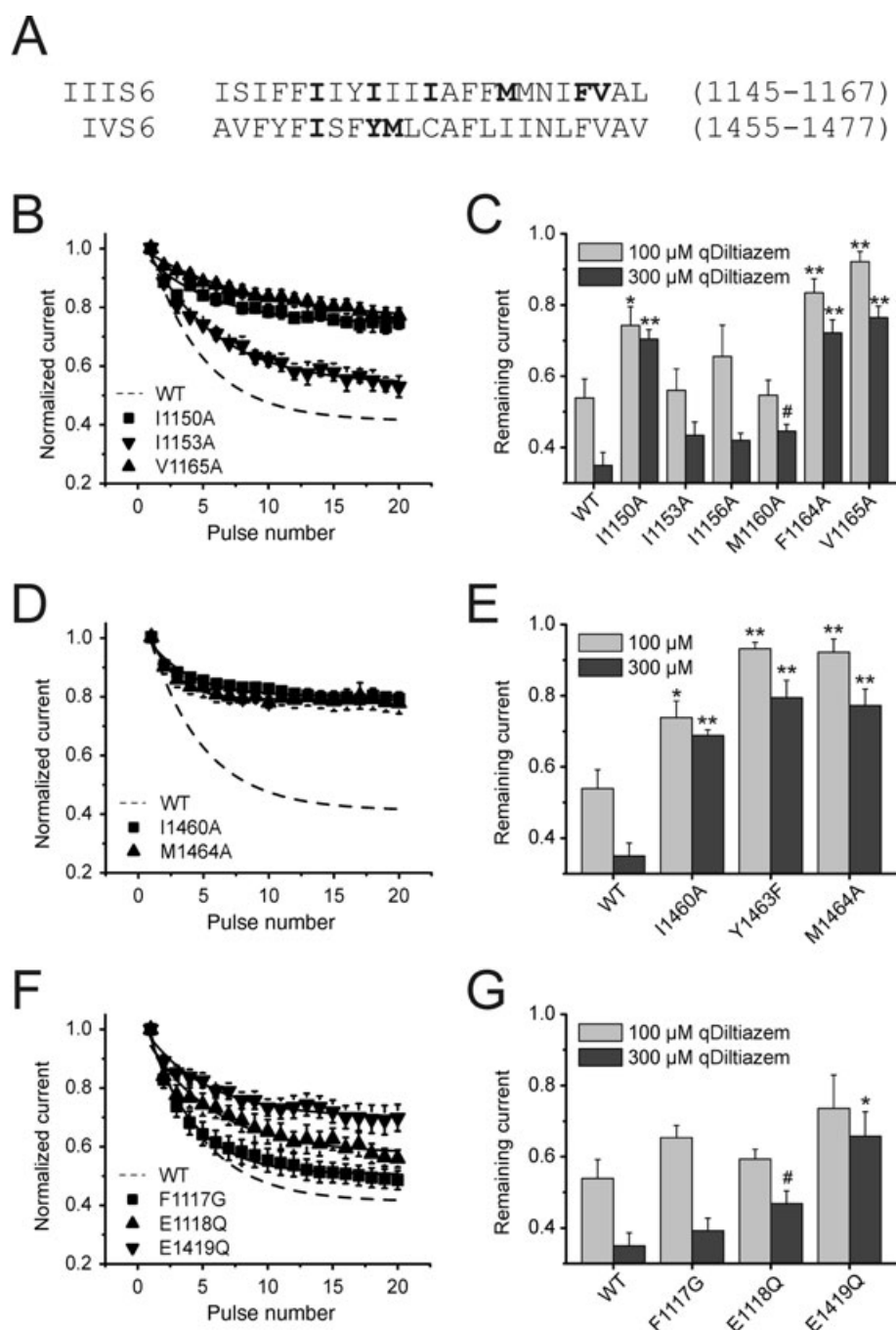
Figure 3

Mutations of the putative d-*cis*-diltiazem binding site affect I_{Ba} inhibition by intracellularly applied quaternary derivative of d-*cis*-diltiazem (qDil). (A) Amino acid sequence of the transmembrane segments IIIS6 and IVS6 of the $Ca_V1.2$ α_1 subunit. Putative diltiazem binding determinants are highlighted. (B) Peak current decay in mutants I1150A, I1153A and V1165A channels induced by 300 µM quaternary diltiazem in the pipette solution (protocol as in Figure 1). (C) Remaining currents after 20 pulses in wild-type (WT) and the indicated IIIS6 mutants. Asterisks denote that the steady-state block value for quaternary diltiazem of the indicated mutant channel is significantly different from that of WT (Student's *t*-test: *$P < 0.05$, **$P < 0.01$, #$P = 0.057$). (D) Use-dependent inhibition of I460A and M1464A channels by 300 µM of qDil in the pipette solution. (E) Remaining currents of WT $Ca_V1.2$ and the indicated IVS6 mutants. Asterisks indicate that the steady-state block value for quaternary diltiazem of the indicated mutant channel is significantly different from that of WT (Student's *t*-test: *$P < 0.05$, **$P < 0.01$). (F) Use-dependent inhibition of selectivity filters mutants F1117G, E1118Q and E1419Q by 300 µM qDil in the pipette solution. (G) Remaining currents after 20 pulses in WT and the indicated $Ca_V1.2$ mutants in 100 and 300 µM qDil in the pipette. Asterisks indicate where there is a significant difference between the steady-state block of the indicated mutant channel and the WT (Student's *t*-test: *$P < 0.05$, #$P = 0.057$). The broken lines in (B, D and F) represent peak current inhibition in wild-type (taken from Figure 1A). Channel block in (C, E and G) was estimated by subtracting 'steady state' inhibition after 20 pulses in drug-free solution (Table 1) from channel block induced by 100 µM or 300 µM of qDil.
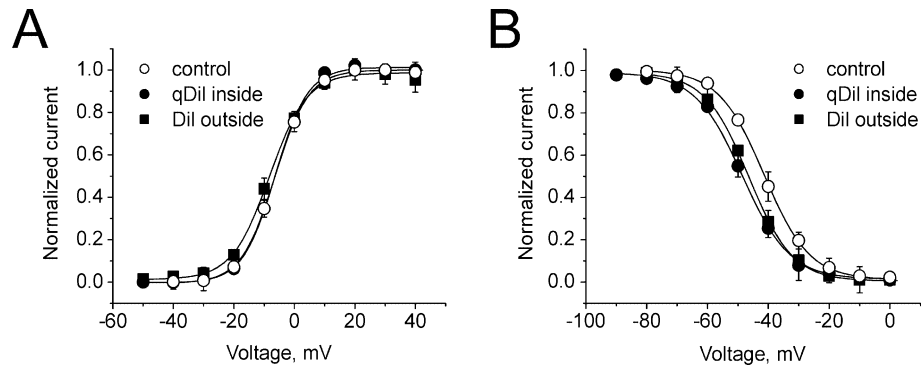
Figure 4

Changes in channel gating induced by d-*cis*-diltiazem (Dil) and quaternary derivative of d-*cis*-diltiazem (qDil). Steady-state activation (A) and inactivation (B) of wild-type (WT) in the absence (control) or presence of 300 μM qDil applied from intracellular side or 300 μM of Dil applied by bath perfusion (see Table 2 for parameters of the Bolzmann distributions).

Table 2

Effects of quaternary derivative of d-*cis*-diltiazem (qDil) and d-*cis*-diltiazem (Dil) on voltage-dependent gating of $Ca_V1.2$

Wild-type	$V_{0.5,act}$, mV	k_{act}, mV	$V_{0.5,inact}$, mV	k_{inact}, mV	r_{1000}, %
Control	-6.4 ± 0.7	5.6 ± 0.6	-41.4 ± 1.0	7.4 ± 0.9	69 ± 6
300 μM qDil (intracellular)	-6.3 ± 0.7	5.3 ± 0.7	-48.5 ± 0.9	7.7 ± 0.8	44 ± 11
300 μM Dil (extracellular)	-8.2 ± 0.8	6.2 ± 0.7	-46.4 ± 1.2	7.2 ± 1.1	38 ± 10

Midpoints and slope factors of the activation and inactivation curves and remaining current after 1000 ms pulse (r_{1000}) at 0 mV pulse ($n = 3–6$).
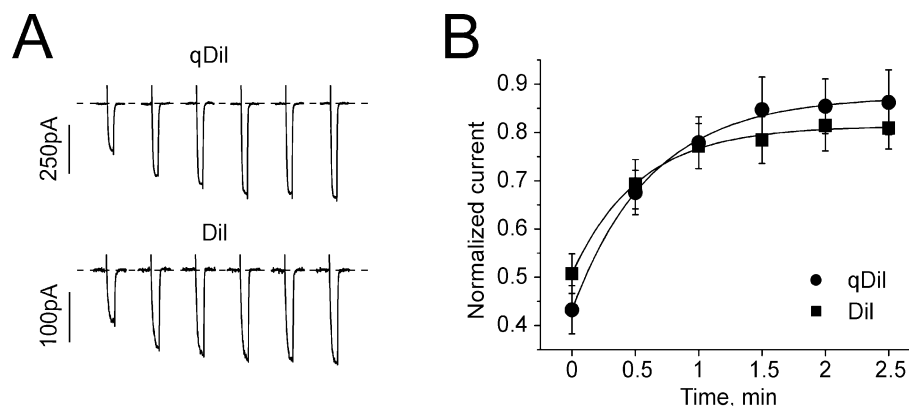

Figure 5

Recovery of wild-type $Ca_V1.2$ from block by intracellularly applied quaternary derivative of d-*cis*-diltiazem (qDil) and extracellularly applied d-*cis*-diltiazem (Dil). (A–B) Recovery from block by 300 μM intracellular quaternary or 300 μM extracellular tertiary diltiazem at −80 mV holding potentials. Block was elicited by a standard conditioning train of 20 pulses in the presence of qDil and recovery monitored by applying short (20 ms) test pulses at different times after the train. The mean time constants of recovery from block by Dil and qDil were 32.3 ± 5.2 ($n = 7$) and 37.1 ± 4.9 ($n = 9$) respectively.

modulating role of channel inactivation in block by diltiazem was revealed in studies with mutant and chimerical $Ca_V1.2$ constructs (Berjukow *et al.*, 1999; Motoike *et al.*, 1999; Dilmac *et al.*, 2003). Like PAAs, diltiazem blocks $Ca_V1.2$ channels in a use-dependent manner (Lee and Tsien, 1983; Hockerman *et al.*, 2000). The molecular mechanism of channel inhibition

and the access path of diltiazem to its receptor site are, however, less well understood. A quaternary BTZ (SQ32,428, Figure 1D) was shown to block L-type channels in BC3H1 cells when applied from the extracellular side of the membrane in a non-use-dependent manner (Hering *et al.*, 1993). Extracellular application of 100 and 300 μM of SQ32,428 on

heterologously expressed $Ca_V1.2$ in the present study confirmed this observation. Tikhonov and Zhorov (2008) hypothesized that access of the 'bulky BTZs' is unlikely to occur through the open activation gate from the intracellular side and proposed a 'side walk' access of BTZ molecules from the extracellular side via the III/IV domain interface to their binding site in the pore. As shown in Figure 1, qDil inhibited I_{Ba} predominantly when applied to the intracellular side of the membrane. The estimated tonic inhibition by intracellularly applied qDil was small (current density of -14.7 ± 0.9 pA·pF^{-1} in control vs. -13.9 ± 1.1 pA·pF^{-1} after first pulse in the presence of 300 µM qDil). Extracellular application (up to 300 µM) did not induce a use-dependent effect (Figure 2C) and produced only a low level of tonic current inhibition (Figure 2D). The more pronounced tonic I_{Ba} inhibition induced by Dil (Figure 2D) contributes to its concentration–inhibition relationship. This is evident from Figure 1B, where stronger I_{Ba} inhibition by Dil was particularly evident at high drug concentrations (See Figure 2D).

Our principle finding that intracellularly applied qDil accesses its binding site through the open activation gate is in line with the data of Smirnov and Aaronson (1998); they suggested that use-dependent current inhibition is induced by the charged form of diltiazem from inside. Furthermore, intracellular channel inhibition by qDil was modulated by four IIIS6 and three IVS6 mutations that have previously been identified as putative diltiazem binding determinants. Selectivity filter mutations less efficiently prevented channel block, which is in line with Dilmac et al. 2003.

Taken together, these data support a scenario where intracellularly applied qDil and extracellularly applied Dil interact with the same or largely overlapping binding pockets in the channel pore (Figure 3).

Intracellular access of the permanently charged qDil to its binding site seems to occur in a very similar way to that previously shown for quaternary PAAs. Quaternary PAAs approach their binding site on $Ca_V1.2$ from the intracellular face of the plasma membrane and repeated channel opening facilitates access of PAAs to the pore region, which explains use-dependent block (Hescheler et al., 1982; Berjukov et al., 1996; Beyl et al., 2007). The access path of charged 1,4 DHPs occurs, however, via a pathway from the extracellular site of the membrane. Amlodipine in its ionized form and the permanently charged quaternary DHP derivative SDZ 207–180 were found to be ineffective when applied intracellularly, suggesting that the DHP receptor site is inaccessible from the intracellular surface, while extracellular application of these compounds resulted in channel block indicating that these antagonists gain access to the receptor site via an extracellular pathway (Kass et al., 1991, see Hockerman et al. 1997 for review). It is tempting to speculate that DHPs reach their receptor determinants in the pore via the 'side walk' access proposed by Tikhonov and Zhorov (2008).

Similar state-dependency of Cav1.2 inhibition by qDil and Dil

High-affinity binding to open and inactivated channel states are important characteristics of use-dependent channel blockers. In order to analyse drug access via the intracellular channel mouth, we have co-expressed the α_1 subunit of Cav1.2 with the β_{2a} subunit, which is known to prolong the open state by minimizing channel inactivation. As shown in Figure 1C and D, the absence of inactivation during short pulses did not prevent use-dependent channel block suggesting access of qDil to its binding site via the open gate. Block development was slow and equilibrated at 300 µM during 15 pulses (Figure 1A). Slow block development is also evident from the acceleration of the current decay with 300 µM qDil in the pipette (Figure 1D) and the non-significant changes in the steady-state activation curve (Figure 4A) (see also Lee and Tsien, 1983). However, channel inhibition is modulated by inactivation, as evident from the shifts of the availability curves in Figure 4B (see also Zhang et al., 2010).

Accumulation of channel inhibition during a pulse train, as illustrated in Figure 1A, depends on channel recovery between pulses. Recovery from use-dependent block by qDil and Dil was found to be very similar [Figure 5, τ(qDil) = 37.1 $\pm$ 4.9 s vs. τ(Dil) = 32.3 $\pm$ 5.2 s]. Similar recovery from block and similar apparent affinities [IC_{50}(Dil) = 95 $\pm$ 5 µM and IC_{50}(qDil) = 85 $\pm$ 9 µM] support the hypothesis that both compounds interact with identical or largely overlapping binding determinants in the channel pore.

The differences in tonic block observed for Dil and qDil warrants further research. The negligible 'intracellular tonic I_{Ba} inhibition' induced by intracellular qDil (current density of -14.7 ± 0.9 pA·pF^{-1} in control vs. -13.9 ± 1.1 pA·pF^{-1} after first pulse in the presence of 300 µM qDil) suggests that the charged form induces predominantly use-dependent block, while the neutral form may be responsible for tonic inhibition (see also Smirnov and Aaronson, 1998). Access of the neutral form of Dil to its binding determinants in the pore via the 'side walk' access (Tikhonov and Zhorov, 2008) cannot be excluded.

Conclusions and outlook

Data from the present study demonstrate intracellular access of quaternary (membrane-impermeable) diltiazem and the interaction of qDil with determinants of the binding pocket previously identified for tertiary diltiazem (Hering et al., 1996; Hockerman et al., 2000; Dilmac et al., 2003). Quaternary diltiazem accesses its binding determinants via the inner channel mouth in a similar manner as was previously found with quaternary PAAs. Our data suggest that use-dependent block of $Ca_V1.2$ by diltiazem occurs predominantly via the open channel conformation.

Our study also permits new insights into the structure–activity relationship of this therapeutically important drug. A structurally related BTZ (SQ32,428) had no effect when applied from the cytosolic side (Figure 2A and C, see also Hering et al., 1993). Compared with SQ32,428, the C_5 of qDil is replaced by a sulphur atom and the trifluoromethyl group in position C_6 is substituted by a hydrogen atom. Additionally, the methyl group of SQ32,428 in position C_3 is replaced by an acetoxy group (Figure 2B). Any of these apparently small structural differences may be essential for interaction of Dil with its intracellularly or extracellularly accessible binding sites. Tikhonov and Zhorov (2008) proposed an interesting concept as to how the functional groups of BTZ may interact with individual amino acid residues in the pore. Derivatives of quaternary diltiazem (with individually replaced moieties) may thus represent interesting tools for investigating the molecular basis of use-dependent drug interactions with intracellular accessible binding determinants.

Acknowledgements

Conflicts of interest

None.

References

Berjukov S, Aczel S, Beyer B, Kimball SD, Dichtl M, Hering S et al. (1996). Extra- and intracellular action of quaternary devapamil on muscle L-type Ca(2+)-channels. Br J Pharmacol 119: 1197–1202.

Berjukow S, Gapp F, Aczel S, Sinnegger MJ, Mitterdorfer J, Glossmann H et al. (1999). Sequence differences between alpha1C and alpha1S Ca2+ channel subunits reveal structural determinants of a guarded and modulated benzothiazepine receptor. J Biol Chem 274: 6154–6160.

Beyl S, Timin EN, Hohaus A, Stary A, Kudmac M, Guy RH et al. (2007). Probing the architecture of an L-type calcium channel with a charged phenylalkylamine: evidence for a widely open pore and drug trapping. J Biol Chem 282: 3864–3870.

Catterall WA (2000). From ionic currents to molecular mechanisms: the structure and function of voltage-gated sodium channels. Neuron 26: 13–25.

Catterall WA, Perez-Reyes E, Snutch TP, Striessnig J (2005). International Union of Pharmacology. XLVIII. Nomenclature and structure-function relationships of voltage-gated calcium channels. Pharmacol Rev 57: 411–425.

Dilmac N, Hillard N, Hockerman GH (2003). Molecular determinants of Ca2+ potentiation of diltiazem block and Ca2+-dependent inactivation in the pore region of cav1.2. Mol Pharmacol 64: 491–501.

Ellis SB, Williams ME, Ways NR, Brenner R, Sharp AH, Leung AT et al. (1988). Sequence and expression of mRNAs encoding the alpha 1 and alpha 2 subunits of a DHP-sensitive calcium channel. Science 241: 1661–1664.

Fleckenstein A, Fleckenstein-Grun G (1980). Cardiovascular protection by Ca antagonists. Eur Heart J 1 (Suppl. B): 15–21.

Hamill OP, Marty A, Neher E, Sakmann B, Sigworth FJ (1981). Improved patch-clamp techniques for high-resolution current recording from cells and cell-free membrane patches. Pflugers Arch 391: 85–100.

Hering S, Savchenko A, Strubing C, Lakitsch M, Striessnig J (1993). Extracellular localization of the benzothiazepine binding domain of L-type Ca2+ channels. Mol Pharmacol 43: 820–826.

Hering S, Aczel S, Grabner M, Doring F, Berjukow S, Mitterdorfer J et al. (1996). Transfer of high sensitivity for benzothiazepines from L-type to class A (BI) calcium channels. J Biol Chem 271: 24471–24475.

Hescheler J, Pelzer D, Trube G, Trautwein W (1982). Does the organic calcium channel blocker D600 act from inside or outside on the cardiac cell membrane? Pflugers Arch 393: 287–291.

Hockerman GH, Peterson BZ, Johnson BD, Catterall WA (1997). Molecular determinants of drug binding and action on L-type calcium channels. Annu Rev Pharmacol Toxicol 37: 361–396.

Hockerman GH, Dilmac N, Scheuer T, Catterall WA (2000). Molecular determinants of diltiazem block in domains IIIS6 and IVS6 of L-type Ca(2+) channels. Mol Pharmacol 58: 1264–1270.

Hohaus A, Beyl S, Kudmac M, Berjukow S, Timin EN, Marksteiner R et al. (2005). Structural determinants of L-type channel activation in segment IIS6 revealed by a retinal disorder. J Biol Chem 280: 38471–38477.

Kass R, Arena JP, Chin S (1991). Block of L-type calcium channels by charged dihydropyridines: sensitivity to side of application and calcium. J Gen Physiol 98: 63–75.

Kraus RL, Hering S, Grabner M, Ostler D, Striessnig J (1998). Molecular mechanism of diltiazem interaction with L-type Ca2+ channels. J Biol Chem 273: 27205–27212.

Lee KS, Tsien RW (1983). Mechanism of calcium channel blockade by verapamil, D600, diltiazem and nitrendipine in single dialysed heart cells. Nature 302: 790–794.

Mathias RT, Cohen IS, Oliva C (1990). Limitations of the whole cell patch clamp technique in the control of intracellular concentrations. Biophys J 58: 759–770.

Motoike HK, Bodi I, Nakayama H, Schwartz A, Varadi G (1999). A region in IVS5 of the human cardiac L-type calcium channel is required for the use-dependent block by phenylalkylamines and benzothiazepines. J Biol Chem 274: 9409–9420.

Schulla V, Renström E, Feil R, Feil S, Franklin I, Gjinovci A et al. (2003). Impaired insulin secretion and glucose tolerance in beta cell-selective Ca(v)1.2 Ca2+ channel null mice. EMBO J 22: 3844–3854.

Sinnegger-Brauns MJ, Hetzenauer A, Huber IG, Renström E, Wietzorrek G, Berjukov S et al. (2004). Isoform-specific regulation of mood behavior and pancreatic beta cell and cardiovascular function by L-type Ca 2+ channels. J Clin Invest 113: 1430–1439.

Smirnov SV, Aaronson PI (1998). pH-dependent block of the L-type Ca2+ channel current by diltiazem in human mesenteric arterial myocytes. Eur J Pharmacol 360: 81–90.

Striessnig J (1999). Pharmacology, structure and function of cardiac L-type Ca(2+) channels. Cell Physiol Biochem 9: 242–269.

Striessnig J, Murphy BJ, Catterall WA (1991). Dihydropyridine receptor of L-type Ca2+ channels: identification of binding domains for [3H](+)-PN200-110 and [3H]azidopine within the alpha 1 subunit. Proc Natl Acad Sci U S A 88: 10769–10773.

Striessnig J, Grabner M, Mitterdorfer J, Hering S, Sinnegger MJ, Glossmann H (1998). Structural basis of drug binding to L Ca2+ channels. Trends Pharmacol Sci 19: 108–115.

Tikhonov DB, Zhorov BS (2008). Molecular modeling of benzothiazepine binding in the L-type calcium channel. J Biol Chem 283: 17594–17604.

Triggle DJ (2007). Calcium channel antagonists: clinical uses – past, present and future. Biochem Pharmacol 74: 1–9.

Uehara A, Hume JR (1985). Interactions of organic calcium channel antagonists with calcium channels in single frog atrial cells. J Gen Physiol 85: 621–647.

Zhang HY, Liao P, Wang JJ, Yu de J, Soong TW (2010). Alternative splicing modulates diltiazem sensitivity of cardiac and vascular smooth muscle Ca(v)1.2 calcium channels. Br J Pharmacol 160: 1631–1640.